Surface Science 76 (1978) 311–322
© North-Holland Publishing Company

LOW ENERGY ION IMPACT PHENOMENA ON SINGLE CRYSTAL SURFACES

Don E. HARRISON, Jr. and P.W. KELLY
Department of Physics and Chemistry, Naval Postgraduate School, Monterey, California 93940, USA

Barbara J. GARRISON
Department of Chemistry, University of California, Berkeley, California 94720, USA

and

Nicholas WINOGRAD *
Department of Chemistry, Purdue University, W. Lafayette, Indiana 47907, USA

Received 14 February 1978; manuscript received in final form 14 April 1978

The dynamics of a solid bombarded by a 600 eV Ar^+ ion have been studied classically by computer simulation. The model uses a crystallite of about 250 atoms described by pair potentials derived from elastic constants and which reproduce the surface binding energy of the solid. The relative calculated yield of secondary atom emission from the three low index faces of Cu follow the previously determined experimental order (111) > (100) > (110). We find major differences in the sputtering mechanisms for these faces. On (110), the impacted atom is ejected most frequently, while on (111) and (100) it almost never leaves the solid. We report the energy distribution of the sputtered particles for each face. The simulation successfully predicts the shape of the curve including the low energy maximum which is observed experimentally near 2 eV. In addition our model shows that many low energy atoms attempt to leave the crystal but are subsequently trapped to the solid at large distances from their original sites. This mechanism of radiation enhanced diffusion inevitably occurs in conjunction with sputtering or any other heavy secondary particle emission or scattering process.

1. Introduction

The interaction of ion beams with solid surfaces has been a general topic of study for several decades. Of special recent interest is the use of low energy ion beams (<2000 eV) in the analysis of surface structure. With these methods, either the secondary ions produced by the primary impact are analyzed by a mass spectrometer as in secondary ion mass spectrmetry (SIMS) or the energy of the

* Presently on leave at the Materials and Molecular Research Division, Lawrence Berkeley Laboratory, Berkeley, California 94720, USA.

reflected primary ion is measured electrostatically as in ion scattering spectrometry (ISS). The generation of surface structural information seems feasible from several early studies [1–7], but the detailed mechanisms that give rise to the secondary processes are still unclear.

Understanding of these mechanisms depends upon the ability to calculate the dynamics of a large number of atoms, which surround the impact site, after they have received the initial momentum of the primary ion. The ionization mechanism of the emitted atom or molecule must then be known, since the ionization probability largely determines the intensity of the observed species.

Here we focus our attention on the first aspect of this problem; that is, an investigation of the details of the secondary collision cascade generated in the solid. We are particularly concerned with the structure-sensitive aspects of secondary particle emission since they represent a new dimension in the elucidation of surface structure. Although uncertainties about the ionization process remain, the conclusions concerning the role of surface structure in the momentum deposition process should be of general utility as a foundation for the understanding of a variety of ion bombardment and ion emission experiments.

Many theoretical models have been developed to explain the molecular dynamics resulting from these collisions. The approach developed by one of us (DEH) over the last fifteen years involves a numerical integration of the classical laws of motion to obtain the positions of all particles in a several hundred atom microcrystallite subsequent to the primary ion impact [8–10]. This method has led to an appreciation of the important ways in which crystal structure influences sputtering and the complexity of the collision cascades generated in the solid, and has discouraged us from further development of analytical expressions based on necessarily gross approximations.

In this paper, we examine in detail the structure-sensitive influences of secondary particle emission by comparing the dynamics resulting from the 600 eV Ar^+ ion bombardment of the 3 low index faces of Cu. By using a larger microcrystallite and by choosing an ion beam of much lower energy than in previous studies [9], we believe that containment of all important dynamical processes has been achieved. These modifications increase the insight into how the crystal structure and orientation influence secondary particle emission gained by the simulation method. We now have successful correlation to experiment for a wide variety of observables including relative sputtering yields, secondary particle angular distributions [8] as well as the secondary particle energy distribution. For example, the calculations clearly demonstrate that the exposed nature of a first layer atom in the (110) crystal enhances its ejection probability when it is struck by a primary ion. The target atoms on the (111) face and the (100) face, on the other hand, are always driven down into the crystal and almost never leave the solid. We also demonstrate that the energy distribution of ejected atoms follows precisely the experimental curve for Ar^+–Cu and that many slow moving atoms can be trapped by the surface at some distance from their original position.

2. Description of calculation

The dissipation of momentum which results when an energetic ion strikes a solid is modeled using classical dynamics. The positions and velocities of the primary ion and all the lattice atoms are developed in time during the trajectory or collision cascade. The cascade is terminated when the momentum has dissipated through the microcrystallite and no more atoms can be ejected. In practice we stop the calculation when the most energetic particle remaining in the crystal has 2 eV of kinetic energy. The final positions and velocities are used to determine yields, the energy distribution, possible multimer formation, and the angular distribution of ejected atoms.

The integration scheme [8,9], the bulk solid potential [9,10], and the ion-solid potential have been described previously [10]. We chose to use a primary ion energy of 600 eV at normal incidence. Approximately 100 trajectories were run on each crystal face to sample a representative area of the surface [9]. The mass of the primary ion is that of argon and of the solid atoms is that of copper.

The motion of atoms in the microcrystallite subsequent to the initial ion impact extends over many lattice sites, even at 600 eV. Since we wish to generate sputtering yields from the three crystal faces that can be compared quantitatively, containment of the collision cascades is critical. We investigated these effects by systematically increasing the crystallite size until the sputtering yield becomes independent of size.

To test for the influence of crystal size on the dynamics, an impact point was chosen which generated a relatively large number of secondary particles. We worked with a primary ion energy greater than that used in the yield studies. The largest crystallite examined fails to contain the entire cascade event and appreciable movement of the edge atoms is detected before the last atom leaves the surface. On the other hand, the significant features of the dynamics are not altered beyond a certain crystal size. Of particular interest is that the number of layers is much less important in influencing the dynamics than the size of the surface layer [8,9]. Based on the above criteria we selected a microcrystallite which is a reasonable compromise between momentum containment and computer execution time, but which did not compromise total yield values. A typical trajectory on a square (100) crystal containing 4 layers with 60 atoms/layer ($N = 240$) requires about 30 seconds on a CDC 7600 computer. This time increases roughly as N^2.

The analysis of the properties of the ejected particles is complicated by the formation of multimers (multiatom clusters) in the region above the surface [10,13]. For the yield measurements reported in this work, we count all of the particles which leave the surface, independent of multimer formation. The available experimental yield measurements were determined by a target weight loss procedure which is insensitive to multimer formation. For energy distributions, however, the analysis is based only on the monomers, since the experimental measurements consisted of a time analysis of the atomic fluorescence [14]. Our

procedure checks the final positions and velocities of the ejected particles to determine whether a stable multimer (dimer, trimer, etc.) could form [15]. If clustering appears likely, the atoms involved are removed from the energy distribution curve.

3. Sputtering yields for 600 eV Ar^+ on Cu (100), (110) and (111)

The large target crystals, the inclusion of an attractive potential and the use of low energy primary ions makes feasible a relative, quantitative comparison of the sputtering of the three low index faces of copper. Our results are presented in table 1. For each crystal, a representative area is chosen [16], which is characteristic of the target orientation. For normally incident ions all possible impact points can be mapped into this area. The sputtering yield is defined as the average over impact area of the number of atoms ejected per incident ion. The calculated order of the yields is S (111) > S (100) > S (110).

There are no experimental measurements for the yields on single crystal copper at 600 eV. Early measurements by Magnuson and Carlston [17] at 1 keV are certainly in good agreement with our results when normalized to the (100) face, as shown in table 1. We are hesitant to make any detailed comparisons, however, since those experiments involved extensive bombardment of the surface, which is presumed to destroy much of the crystal order. The correct trend of the data is most encouraging.

Much additional information can be gleaned from a more detailed look at the lattice dynamics. A summary of the frequency with which each atom is ejected, is shown in fig. 1 for each crystal face. The most striking feature of this representation is that the target atom, which is struck by the primary ion, is ejected most often on the (110) face but is rarely seen to leave the solid on the (111) or (100) face. The target atom ejects by two mechanisms. First, the primary ion can impact in the open "valley", reflect upward and drive the target atom out from behind. Secondly, the ion can hit the target atom directly causing the target atom to reflect

Table 1
Sputtering yield of 600 eV argon on copper (100), (110) and (111)

Crystal face	Total number of trajectories	Total number of atoms ejected	Sputtering yield	Relative yield	
				Calculated [a]	Experimental [b]
(100)	111	436	3.93	1.00	1.0
(110)	121	429	3.54	0.90	0.5
(111)	108	700	6.48	1.65	1.3

[a] Normalized to the (100) face.
[b] Measured at 1 keV by weight loss, normalized to the (100) face.

off the open "valley" and eject. The example on (110) is the only one in which there is a high probability that the target is sputtered. These mechanisms may be particularly important in the sputtering of chemisorbed adatoms on the target surface. This simple comparison is a spectacular example of the strong structure sensitivity of the momentum deposition process.

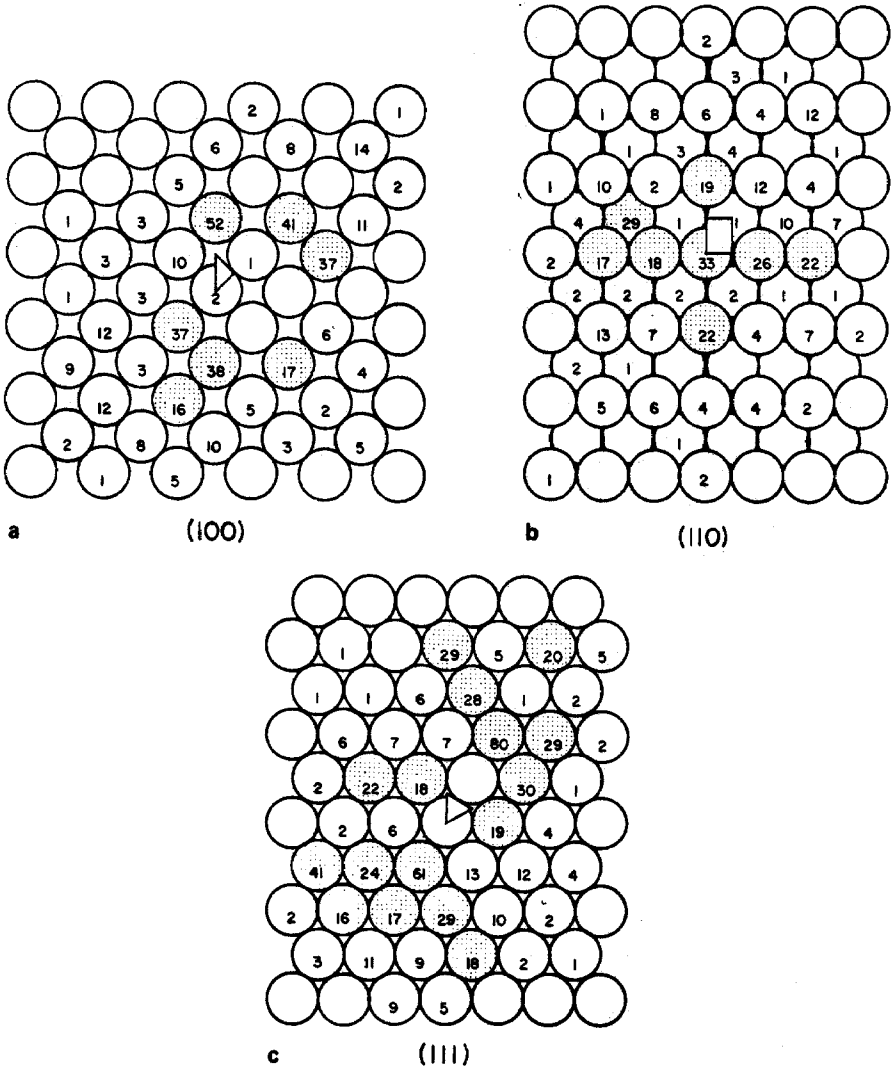

Fig. 1. Emission of atoms from bombardment of copper by 600 eV Ar^+ ions. (a) is Cu (100), (b) is Cu (110), and (c) is Cu (111). The numbers in the atoms refer to the percentage of events in which the particular atom was ejected . The shaded atoms are the ones ejected most frequently. The representative area for each face has been indicated.

A second important mechanism is the propagation of momentum down close packed rows of atoms. This mechanism, discussed by Harrision and Delaplain [10], is particularly evident on the (100) surface. For the moment, use the probability of ejection as labels. Then on the (100) surface "2" is the target atom and the alternation effect along the "37"–"41" row is apparent. This mechanism is obscured on the other surfaces by the convolution of the effects of many impact points and other mechanism. It can be picked out on the (111) surface, see the "61", "80", "20" line, but is not obvious from casual inspection. It is almost totally obscured on the (110) surface unless the results from individual impact points are examined separately.

Qualitative insight into the degree of surface damage can be gained from the data displayed in fig. 1. The distribution of ejected atoms as a function of their original distance from the target atom is displayed in fig. 2. On the (100) and (111) faces many atoms are ejected from a ring at some distance from the impact point. On the (100) surface the distribution is narrower than on the (111) surface, because there are fewer possible directions of momentum propagation. On the (110) surface the basic sputtering mechanism is different since, as discussed earlier, a pathway exists for the direct ejection of the target atom. Note that on all three surfaces the damage cross section is nearly 200 $Å^2$ per primary ion.

For all three target orientations, most of the sputtered atoms originate from the surface layer (see table 2). Note that on (100), virtually every atom originates from the first layer, even though the dynamics induces significant movement of atoms 4 layers below the surface. On (110) a fairly large fraction (~25%) of the atoms are ejected from the second layer, which, because of the open structure of the top layer, is also exposed. For (111) approximately 95% of the atoms originate from

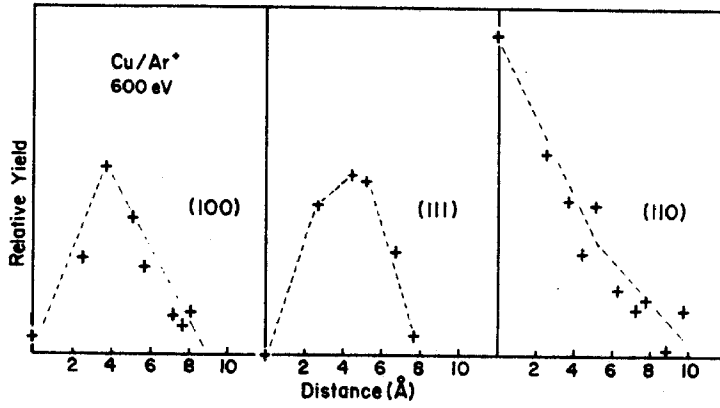

Fig. 2. Relative yield versus distance from target atom for Cu (100), (111) and (110). The points represent the fraction of ejected particles per distance unit. The lines are only meant as a guide to the eye and have no physical significance.

Table 2
Origin of ejected copper atoms resulting from 600 eV normal incidence Ar^+ ion impact

Origin of ejected atom (atomic later number)	Number of ejected atoms		
	(100)	(110)	(111)
1	435	348	672
2	1	79	28
3	0	2	0
4	0	0	0

the first layer. These results support the general assumption about surface sensitivity that experimentalists employing the "static" SIMS technique [1] have used for several years.

The ultimate disposition of the primary ion is also of interest. In this model the retention of the primary ion in the target is readily determined. We find that nearly 22% of the primary argon ions are implanted into the lattice for (110) while only 8 and 14% remain in the lattice for the (100) and (111) faces, respectively. Clearly, the existence of open channels in (110) allows easier penetration while the closer packing of the other faces makes this penetration more difficult.

4. Energy distribution of sputtered atoms

The variation of the energy distribution with crystal orientation and morphology represents a potential new experimental probe to elucidate surface structure. For example, several workers have proposed that the maximum intensity of emitted atoms occurs near the surface binding energy of the solid [18–20]. In this section we compare the predictions of our model to the experimental data, and correlate our results with detailed information derived from the study of individual cascades.

The calculated energy distribution of particles emitted from the (100), (110), (111) faces and their sum (termed "polycrystalline") are shown in fig. 3, again for 600 eV Ar^+ ion impact. These distributions are equivalent to those which would be obtained in an ideal experiment in which all emitted particles are captured and analyzed. There are no significant differences in either shape or maximum location among the three curves. The slight variation in the Cu (111) distribution may be a manifestation of the removal of those atoms bound into clusters. When the three distributions are plotted together in the "polycrystalline" curve, the similarity is even more apparent.

The experiments which most nearly correspond to these distributions were performed by time of flight analysis of the atom velocities from Cu (110) by Stuart and Wehner [14]. These data and computed results are plotted together in fig. 3.

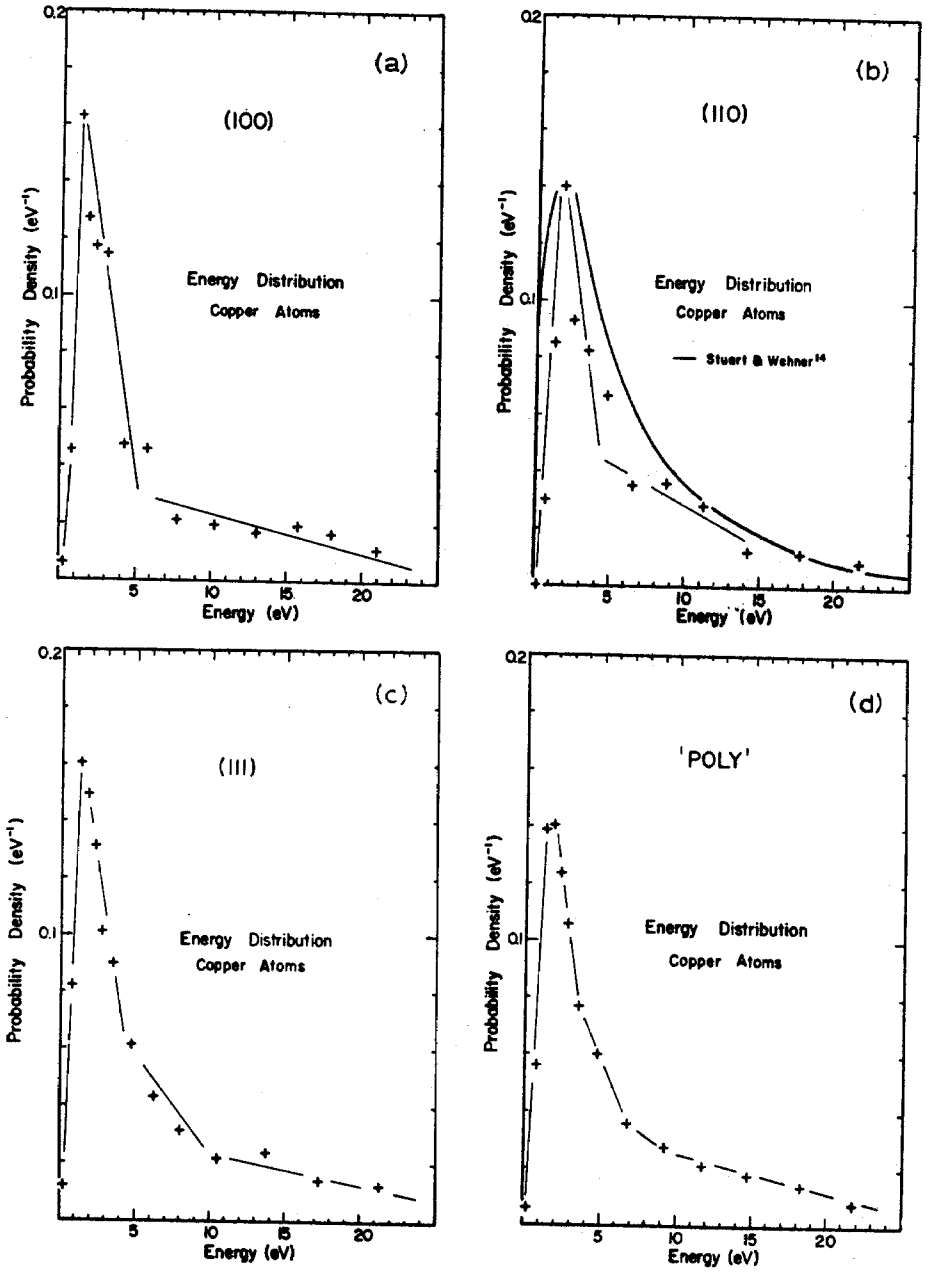

Fig. 3. Energy distribution for 600 eV Ar^+ ion on (100), (110), (111) and "polycrystalline" copper. The "polycrystalline" distribution was obtained by adding the distributions for the 3 faces. The solid line drawn in the (110) figure is the distribution as measured by Stuart and Wehner. The other lines are only intended as a guide and have no physical significance.

The agreement is remarkable. Note that there are *no adjustable parameters* in the calculated distributions, so we have increased confidence that the computed results are reliable, and that insights obtained by careful analysis of individual cascades have value.

Several features of the curve are clearly apparent. The energy distribution starts at zero, peaks at a fairly low value, ~2 eV, and is followed by a drop-off of nearly $1/E$. The calculations also show that the tail of the curve extends beyond 100 eV. The shape in the low energy regime arises from the refraction of atoms traveling across a potential barrier at the surface [11,20]. An atom moving with kinetic energy just equal to this "surface potential" can only escape the solid if it is moving normal to the surface, otherwise it will suffer a reflection and be recaptured by the solid. Thus, only an infinitesimally small fraction of the atoms moving with this energy can escape and their energy after they escape will be zero. This concept is clearly illustrated by our simulations. As shown in fig. 4, conservation of the parallel component of the momentum results in a distribution of atom energy which maximizes at 0. The surface potential which affects the energy associated

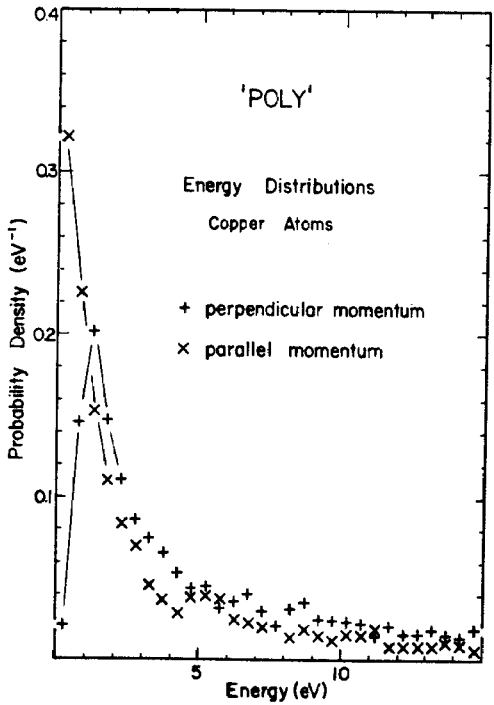

Fig. 4. Energy distributions for the perpendicular and parallel momentum component of the kinetic energy for 600 eV Ar^+ ion on "polycrystalline" copper.

with the perpendicular component of the momentum results in the peaked behavior of the energy distribution curve near 2 eV.

Some insight into the shape of the remainder of the energy distribution curve can be obtained by examination of the cascade dynamics. The atoms ejected with kinetic energy greater than ~10 eV generally are ejected after only 2 or 3 collisions subsequent to the primary impact. Many of the higher energy events result from the upward-downward alternation of momentum down a close-packed row of atoms [10] as discussed in section 3. The atoms with energy between 0 eV and 10 eV however, generally are ejected late in the cascade and result from a long series of collisions which effectively dissipate the momentum over many atoms. Note that these atoms, which comprise the major portion of the total yield, are the result of low energy multiple collision events which are least well handled by the analytic sputtering theories.

5. Radiation enhanced diffusion

The low energy atoms which attempt to leave the solid but have insufficient kinetic energy to overcome the surface potential effectively migrate over the surface. This mechanism contributes to the enhanced movement of atoms about a

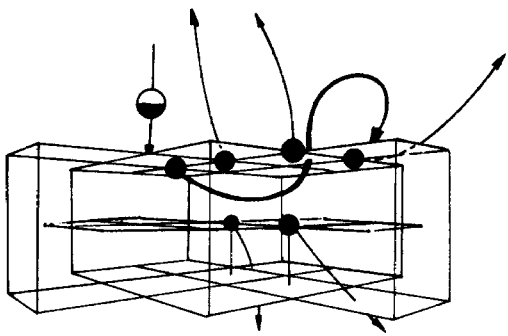

Fig. 5. Pictorial representation of a radiation enhanced diffusion mechanism caused by the trapping of low energy atoms. The incoming ion (half-filled) collides with a surface layer atom (filled) and drives it into the space between the first and second layers of the crystal. As it moves it pushes two atoms from the second plane downward and sputters two atoms from the surface layer. It returns toward the surface, and makes a hard collision with a third surface layer atom, which also is ejected. The atom now moves above the surface plane, but it no longer has sufficient energy to escape the surface potential barrier; so it is trapped by the solid. At the end of the event the recoiling surface layer atom has ejected three other atoms, and remains on the surface approximately 7 Å from its original site. The picture has been greatly simplified so that the important event can be followed. In all layers additional atoms are located at the intersections of the lines. The pictured event occurred in a (100) crystal, but obviously the mechanism need not be limited to that surface.

surface under the influence of ion bombardment. In fig. 5, we focus on the path taken by an atom during a particular collision cascade. In this case the target atom obtains nearly 200 eV of kinetic energy from the collision with the Ar^+ ion, and is driven into the solid. It strikes two atoms in the second layer and reverses direction. As this atom repasses through the first layer, it collides with and ejects two atoms, leaving itself with less than 1 eV of kinetic energy. It's upward energy component is now no longer sufficient to allow it to escape, even though it rises nearly 2.5 Å above the top layer. The atom eventually "turns-around", bounces along the surface and is recaptured by the solid.

In this example, the atom is deposited more than 7 Å from its original position, although it never formally leaves the crystal. We believe this represents a valid mechanism for radiation enhanced diffusion of atoms on a surface. The process essentially involves the trapping of slow-moving atoms as they move with momentum almost parallel to the surface [21,22]. This type of behavior occurs frequently in the cascades we have examined in detail.

6. Conclusions

In this paper, we have compared the consequences of 600 eV Ar^+ ion bombardment on the three low index faces of Cu. The analysis indicates that strong structure-sensitive factors influence the nature of the collision cascade and hence the mechanisms for particle ejection.

The important findings are as follows:

(1) The use of lower energies and larger microcrystallites allows direct comparison of computed and experimental yield ratios. The agreement is satisfying.

(2) Examination of the three primative surfaces of the same target material reinforces the previous conclusion that sputtering is essentially a surface layer phenomenon for these, and presumably other, target orientations. In the process the row-alternation sputtering mechanism has been identified as an important contributor to (111) and (100) surface sputtering, and a new mechanism for particle ejection has been identified on the (110) surface.

(3) Energy distributions have been obtained for the three faces. The distributions are almost identical, which indicates that the underlying distribution within the solid is not strongly orientation dependent; so the difference detected in sputtering from various surfaces are even more clearly identified as the results of surface morphology.

(4) The energy distributions agree well with the limited experimental data available, further enhancing our confidence in the model.

(5) Detailed analysis of cascades has indicated that slow moving recaptured atoms can contribute significantly to radiation enhanced diffusion by redepositing several angstrom units away from their site of origin.

Acknowledgement

The authors thank the National Science Foundation (Grant No. MPS75-9308), the Materials Research Program (Grants No. DMR-72-3-19A04) and the Air Force Office of Scientific Research (Grant No. AF762974) for financial support. On of us (NW) also thanks the J.S. Guggenheim Foundation for a fellowship and the Lawrence Berkeley Laboratory, which is supported by the US Department of Energy, and Professor D.A. Shirley for providing access to their research facilities. Portions of the computations were supported by the Foundation Research Program of the Naval Postgraduate School with funds provided by the Chief of Naval Research.

References

[1] A. Benninghoven, Surface Sci. 35 (1973) 427.
[2] M.L. Yu, Surface Sci. 71 (1978) 121.
[3] M. Barber, J.C. Vickerman and J. Wolstenholine, J. Chem. Soc. Faraday Trans. I, 72 (1976) 40.
[4] P.H. Dawson, Phys. Rev. B15 (1977) 5522.
[5] E. Taglauer, G. Marin, W. Heiland and U. Beitat, Surface Sci. 63 (1977) 507.
[6] S. Prigge, H. Niehus and E. Bauer, Surface Sci. 65 (1977) 141.
[7] A. Shepard, R. Hewitt, W. Baitinger, G.J. Slusser, N. Winograd, G.L. Ott and W.N. Delgass, in: Quantitative Surface Analysis of Materials, ASTM STP 643, Ed. N.S. McIntyre (1978).
[8] D.E. Harrison, Jr., N.S. Levy, J.P. Johnson, III and H.M. Effron, J. Appl. Phys. 39 (1968) 3742.
[9] D.E. Harrison, Jr., W.L. Moore, Jr. and H.T. Holcombe, Radiation effects 17 (1973) 167.
[10] D.E. Harrison, Jr., and C.B. Delaplain, J. Appl. Phys. 47 (1976) 2252.
[11] G.P. Konnen, A. Tip and A.E. DeVries, Radiation Effects 26 (1975) 23.
[12] G.P. Konnen, J. Grosser, A. Waring, A.E. DeVries and J. Kistemaker, Radiation Effects 21 (1974) 171.
[13] H. Oechsner, Appl. Phys. 14 (1977) 43.
[14] R.V. Stuart and G.K. Wehner, J. Appl. Phys. 35 (1964) 1819.
[15] N. Winograd, D.E. Harrison, Jr. and B.J. Garrison, Surface Sci., submitted.
[16] D.E. Harrison, Jr., J.P. Johnson III and N.S. Levy, Appl. Phys. Letters 8 (1966) 33.
[17] G.D. Magnuson and C.E. Carlston, J. Appl. Phys. 34 (1963) 3268.
[18] Z. Sroubek, Surface Sci. 44 (1974) 47.
[19] P.H. Dawson, Surface Sci. 65 (1977) 41.
[20] M.W. Thompson, Phil. Mag. 18 (1968) 377.
[21] M. Shugard, J.C. Tully and A. Nitzan, J. Chem. Phys. 66 (1977) 2534.
[22] B.J. Garrison and S.A. Adelman, Surface Sci. 66 (1977) 253.